Hindawi
Geofluids
Volume 2023, Article ID 7195779, 11 pages
https://doi.org/10.1155/2023/7195779

Research Article

Experimental Study on the Diffusion Radius of Modified Slurry Used in Longwall Overburden Isolated Grouting

Dayang Xuan[1], **Mingwei Zhang**[1], **Jian Li**[1], **Zebin Dong**[1], **Aimaiti Alimu**[1] and **Jialin Xu**[2]

[1]*School of Mines, China University of Mining and Technology, Xuzhou, Jiangsu 221116, China*
[2]*State Key Laboratory Coal Resources and Safe Mining, China University of Mining and Technology, Xuzhou, Jiangsu 221116, China*

Correspondence should be addressed to Jian Li; li_jian@cumt.edu.cn

Received 12 July 2022; Revised 12 December 2022; Accepted 20 December 2022; Published 6 January 2023

Academic Editor: Zhenyuan Yin

The slurry diffusion radius is an important parameter in grouting engineering. In some cases, injection into partial overburden is needed in grouting engineering, and it is thus critical to control the slurry diffusion so as to reduce unnecessary grout take. In an effort to solve such issues in longwall overburden grouting, we proposed the addition of cement as a means of modifying fly ash slurry in order to reduce grout diffusion and grout take. The characteristics of the modified slurry were determined under different water-ash ratios and cement-blending ratios. The cement-blending ratio was found to have a small effect on the density of the slurry but a significant effect on the slurry's precipitation rate and viscosity. The slurry diffusion experimental system was established to study the diffusion radius and consolidation. Results for both the fly ash slurry and the modified slurry revealed a circular diffusion pattern centered around the grouting borehole. The diffusion radius of the modified slurry made with 10% cement was 19.4% lower than that of the fly ash slurry, but its solidification thickness appeared to increase. The modified slurry diffusion had a two-stage effect: a "stability control stage" and a "consolidation control stage." In the consolidation control stage, the diffusion radius of the modified slurry was smaller than that of the fly ash slurry, and this stage was the key to control the diffusion radius of the slurry. Field trials were conducted based on the results of the study, and grout take was reduced effectively. This research provides a theoretical basis for slurry diffusion radius control in longwall grouting.

1. Introduction

The process of longwall mining causes large area movement and destruction of the overburden [1, 2], thereby forming mining-induced fractures inside the overburden [3] that are continuously transmitted upward in order to induce surface subsidence [4–7]. In the process of overburden movement, there is a layer of hard rock (typically called "key strata" in China) that is thicker and can temporarily act as a barrier to the upward transmission of mining-induced fractures, thereby slowing the rate of surface subsidence. If the key layer of overburden is reinforced during longwall mining, surface subsidence can be effectively stopped [8–11].

The overburden isolated grouting method is a highly efficient technology for reducing surface subsidence. Developed as a means of taking advantage of the role that "key strata" play in controlling surface subsidence [12], the method's technical principle lies in constructing several surface boreholes above the longwall workface down to certain key strata. During mining, the slurry is filled into the mining-induced fissure under the key strata through the surface boreholes at high pressure, and the filling slurry forms a support structure that maintains the stability of the key strata and controls the surface subsidence [13–15]. Commonly, the slurry used in the overburden isolated grouting engineering is fly ash slurry, for it is a solid waste in the coal mine area. This technology has been successfully applied in a few coal mines in China with the goal of protecting surface buildings and infrastructures [16–19]. In longwall grouting practice, it is common for some longwall panels to be only partially covered by buildings; therefore, protecting these buildings against mining subsidence can often be achieved by only partially grouting the overburden area under the buildings.

Traditionally, the slurry used in the overburden isolated grouting project is made of fly ash particles mixed with water [20]. The diffusion radius and thickness distribution of the fly ash slurry have been discussed in previous studies. For example, the slurry diffusion radius of a single borehole in the injection of a longwall panel has been determined using the field multihole method at a Chinese coal mine; it was found that the grout diffusion radius was up to 220 m [21]. In addition, researchers have also carried out relevant experimental studies and proposed distribution models for the end-state thickness distribution of the filled slurry [22, 23]. This model has additionally been applied to grouting design [24, 25]. Under local injection conditions, fly ash slurry may exceed the expected control range due to its large diffusion radius, which significantly increases the amount of filling material and reduces the efficiency of grout filling. Therefore, the fly ash slurry needs to be modified in order to reduce its diffusion radius.

Studies on slurry modification methods and grout diffusion control are common in the field of fractured rock grouting [26–28], but the studied fracture scale and engineering context differ greatly from those applicable to grouting injection into the overburden of isolated panels during longwall mining. In this case, the filling space is the mining-induced fractures, which are far beyond the millimeter-scale filling space used in fractured rock injection. Meanwhile, the filling slurry used in the field of fracture body injection is usually a cement slurry or a chemical slurry [29–31]. Generally, its purpose is to increase the groutability and diffusivity of the slurry, but the modification cost is higher [32–35]. Therefore, significant differences exist between the two engineering contexts. In the overburden isolation grout filling project, the injection ratio (i.e., the ratio of the final compact fill volume of injection to the extraction volume) can be greater than 50%, and the amount of filling material is vast such that it is necessary to use the easily available and inexpensive modified materials to modify the pulverized coal slurry. Therefore, the slurry modification method and the diffusion radius in the fractured rock cannot be directly applied to overburden isolation injection.

The present paper proposes a method of mixing a certain percentage of cement into a fly ash slurry in order to make a modified fly ash slurry and then using the curing effect of cement to reduce the diffusion radius of the fly ash slurry. An experimental study was undertaken in order to determine the basic characteristics of the modified slurry. As part of this study, experimental and field research was conducted on the diffusion radius of the modified slurry, and the mechanism of action of the modified slurry in controlling the diffusion radius was explored.

2. Materials and Methods

During grouting, injection into the overburden of the longwall panel is usually evaluated based on basic parameters such as the density, stability, and rheology of the slurry. Five slurries with differing water-ash ratios (1.2, 1.4, 1.6, 1.8, and 2.0) were selected. The bulk density and density of the fly ash used are 0.54 t/m^3 and 2.47 t/m^3, respectively. The particle size distribution D50 is 16.82 μm. The 45 μm square sieve residue of the fly ash is 11.16%. Cement-mixing ratios of 10%, 20%, 50%, and 80% in the dry fly ash were controlled when making the modified fly ash slurry; the cement is the 32.5R ordinary Portland cement. Differences in density, precipitation rate, and viscosity of the modified fly ash slurry were measured in order to investigate the effects of the water-ash ratio and the cement-mixing ratio on the basic characteristics of the modified fly ash slurry. The effect of the water-ash ratio and cement mixture on the base properties of the modified fly ash slurry was then discussed.

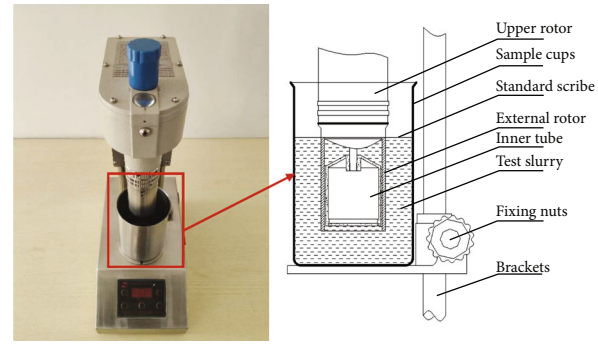

Figure 1: Slurry plastic viscosity test with ZNN-D6X type six-speed rotational viscometer (part of the experimental section).

Subsequently, experimental studies on the diffusion distance of the fly ash slurry and the modified fly ash slurry were conducted separately. The aim was to determine the characteristics of the diffusion, differences in the deposition thickness, and differences in the diffusion radius of the two slurries; to evaluate the control effect of the diffusion radius of the modified fly ash slurry; to reveal the inhibition mechanism of the diffusion radius of the modified fly ash slurry.

2.1. Slurry Parameters Test. In grouting projects, the precipitation rate, which is defined as the ratio of the final deposited volume (i.e., the slurry without the bled water) to the total slurry volume after a static settlement, is usually used to measure the stability of the filled slurry. Modified fly ash slurry manifests as a typical solid-liquid two-stage flow and is thus highly susceptible to water-cement separation. The precipitation rate of the modified fly ash slurry was tested by placing the modified fly ash slurry with water-ash ratios of 2.0, 1.8, 1.6, 1.4, and 1.2 and cement-mixing ratios of 10%, 20%, 50%, and 80%, respectively, into a 100 mL test tube and comparing the differences in precipitation rates.

In order to investigate the time-varying viscosity of the modified fly ash slurry, a modified fly ash slurry with a slurry water-ash ratio of 1.2 and a cement-blending ratio of 10% was selected for viscosity testing with a fly ash slurry with a water-ash ratio of 1.2. As shown in Figure 1, in order to simulate different diffusion times, plastic viscosity was measured using a ZNN-D6X six-speed rotational viscometer after the two above-mentioned slurries had been left to stand for 12 h and 24 h, respectively.

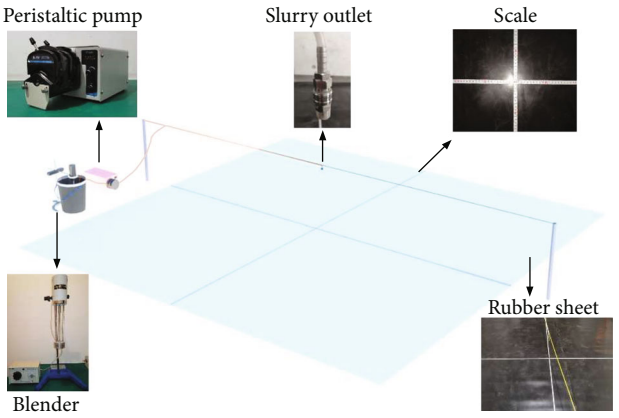

Figure 2: Experimental system of slurry diffusion.

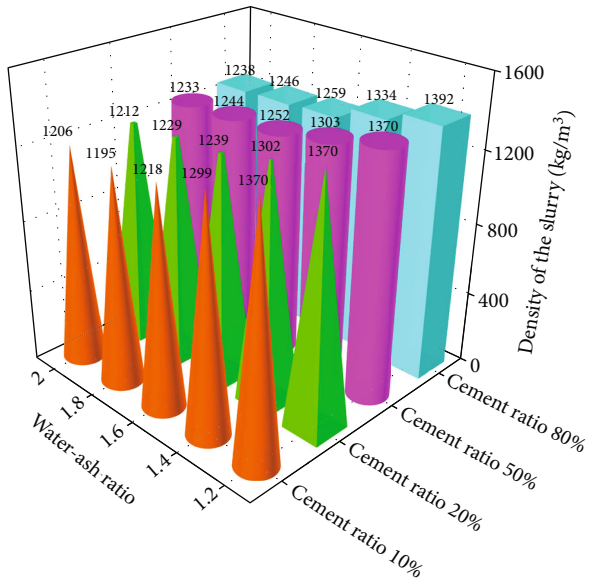

Figure 3: Density of modified fly ash slurry with different water-ash ratios and cement ratios.

2.2. Slurry Flow Experiment. Practically, the range of injection zone is associated with mining geometry (usually with a width of 200-300 m), and the slurry diffusion radius does not exceed 350 m. For the operation of the experiment, the model geometry of 3.5 m × 3.5 m was chosen (i.e., similarity ratio of 1 : 100). Therefore, the slurry diffusion experimental system was constructed according to a geometric similarity ratio of 1 : 100.

As shown in Figure 2, the experimental system consisted of a constant-rate grout pump, a rubber base plate, a slurry barrel, a mixer, a scale, etc. The rubber base plate was used to simulate the rough rock interface in the overburden fracture, and a 3.5 m × 3.5 m base plate was chosen in order to ensure that the slurry diffusion range would be large and the diffusion time long such that the rheological properties of the slurry could be fully reflected. In order to measure the real-time slurry diffusion distance during the filling process, two scales were laid across the center of the bottom plate.

The diffusion of the slurry within the mining-induced fracture is controlled by viscous force and pressure, and the Reynolds number similarity can be used as the similarity criterion. Therefore, the flow similarity ratio is equal to the geometric similarity ratio. Based on the similarity principle, the slurry flow rate was designed to be 30 mL/min. Based on the aforementioned slurry-stability analysis, a modified fly ash slurry with a cement-mixing ratio of 10% was selected for the flow simulation experiment. During the experiment, the slurry was continuously mixed with a mixer in order to protect the slurry from precipitation and deposition.

The rheological properties of the modified and unmodified fly ash slurry needed at least 12~24 h to be fully reflected under static conditions. Therefore, in order to better reflect the differences in flowability and solidification caused by the time-varying viscosity of the modified and unmodified fly ash slurry, the diffusion process of both slurries was measured in uninterrupted 72 h experiments.

3. Results and Discussion

3.1. Characteristics and Parameters of Modified Slurry

3.1.1. Slurry Density. The density of the modified slurry with different water-ash ratio and cement-blending was tested, and the results showed that the density of the modified slurry at a given water-ash ratio slightly increases with the increase of cement-blending ratio. For example, Figure 3 shows that the difference between the density of the modified fly ash slurry with a 10% cement-mixing ratio and the density of the modified fly ash slurry with an 80% cement-mixing ratio was only 1.6% when the water-ash ratio was 1.2, and the difference between the density of the modified fly ash slurry with other water-ash ratio conditions was within 5%. The difference between the density of the slurry with different cement-mixing ratios was within 5%, and the density of the modified fly ash slurry with a water-ash ratio of 1.2 was relatively stable and almost did not change at all with the changing of cement-mixing ratio.

3.1.2. Slurry Stability. The precipitation rate of the modified fly ash slurry with different ratios was found to decrease over time from 0 to 2 h, and the precipitation rate of the modified fly ash slurry basically stabilized after 2 h. When the cement-mixing ratio was the same, the higher the water-ash ratio was, the higher the precipitation rate of the modified fly ash slurry was. Only the modified fly ash slurry with a water-ash ratio of 1.2 had a lower precipitation rate under different cement-mixing ratio conditions, and the precipitation rate remained above 90%.

When the cement-mixing ratio was the same, the higher the water-ash ratio was, the higher the precipitation rate of the modified fly ash slurry was. Only the modified fly ash slurry with a water-ash ratio of 1.2 had a lower precipitation rate under different cement-mixing ratio conditions, and the precipitation rate remained above 90%.

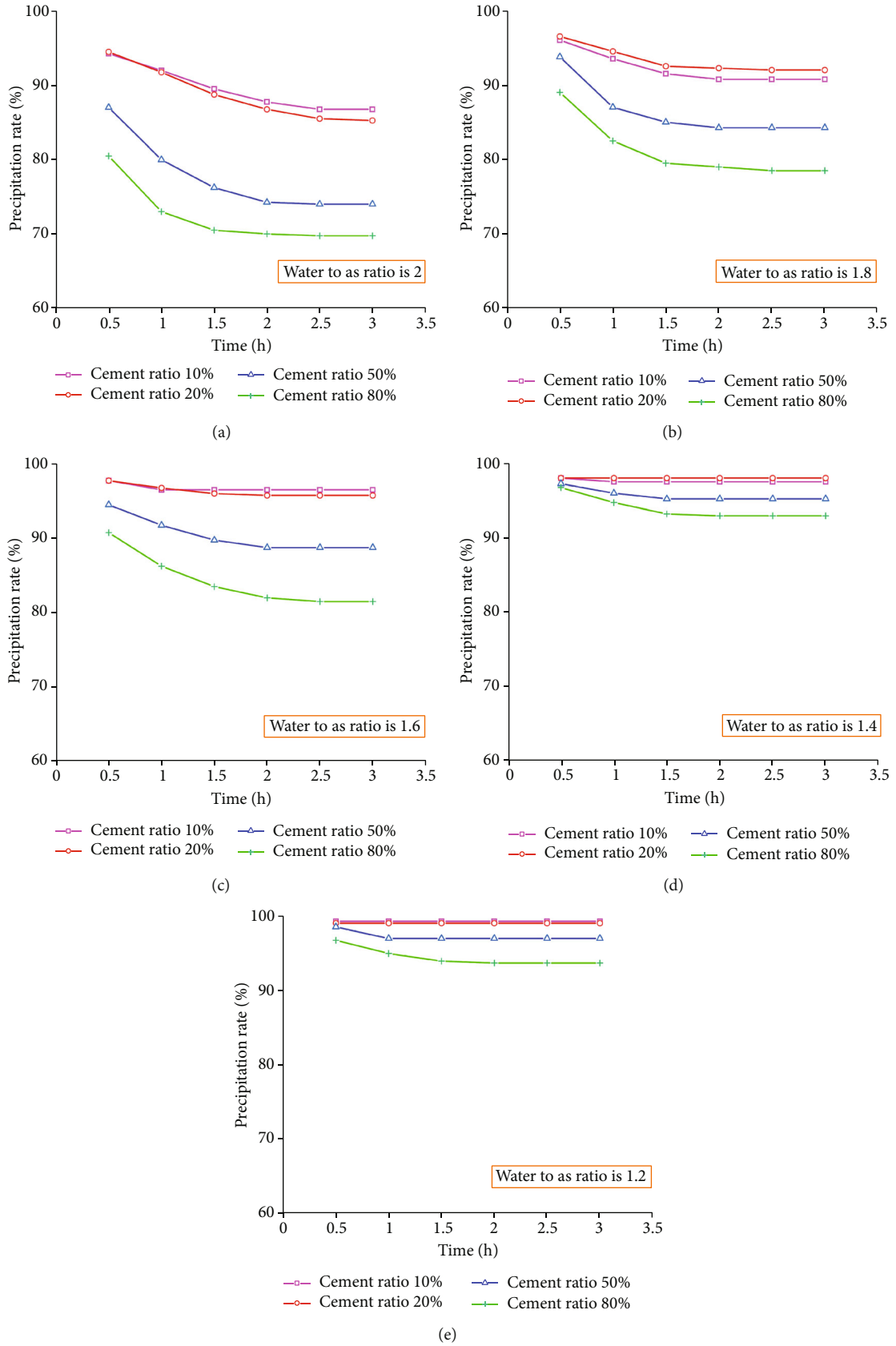

Figure 4: Average slurry precipitation rate corresponding to different water-ash ratios. (a) Water-ash ratio of 2; (b) water-ash ratio of 1.8; (c) water-ash ratio of 1.6; (d) water-ash ratio of 1.4; (e) water-ash ratio of 1.2.

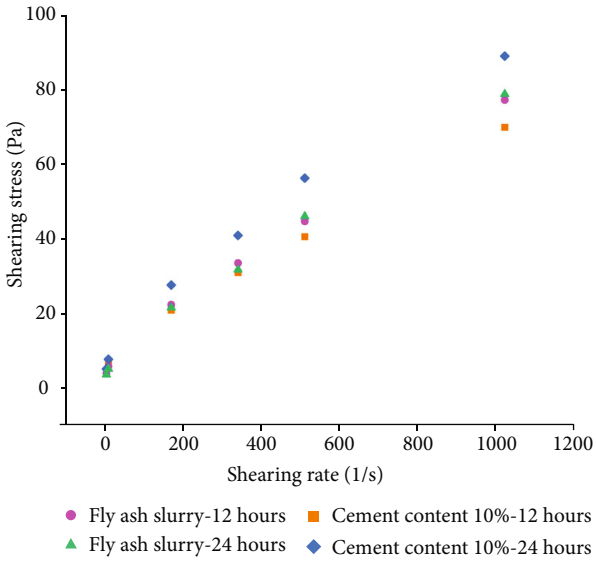

FIGURE 5: Fly ash, modified fly ash slurry (water-ash ratio of 1.2) plastic viscosity.

When the slurry water-ash ratio was the same, the cement-doping ratio was different, but the modified fly ash slurry precipitation rate increased with increasing cement doping. As shown in Figure 4, the difference between the precipitation rate of the slurry with a 10% and 20% mass-doping ratio was very small, and the stability of slurry was good. The difference was more obvious when the cement-blending ratio was 50%, 10%, or 20%, and the precipitation rate was higher when the doping ratio reached 80%. Adding more cement to the pulverized coal slurry clearly significantly increased its precipitation rate, which was not conducive to the flow of the slurry in the mining-induced fractures. Therefore, it was advisable to choose a small amount of cement for modification. The stability difference between the two slurries with 10% and 20% admixture, respectively, was small, and from the perspective of cost reduction, the 10% cement admixture was preferred for the diffusion radius experiments.

3.1.3. Slurry Rheology. Fly ash slurry and modified slurry are both Bingham fluids, and the rheological equations is

$$\tau = \tau_0 + \eta_p \frac{du}{dy}, \quad (1)$$

where τ is the shear stress, τ_0 is the ultimate dynamic shear stress, η_p is the plastic viscosity, and du/dy is the shear rate. The shear stress values at 600, 300, 200, 100, 6, and 3 r/min were measured using a six-speed rotational viscometer, as shown in Figure 5. The measured values were used to plot the relationship between shear rate and shear stress, and the plastic viscosity can be obtained by Equation (1).

The test results revealed that the plastic viscosity of the fly ash slurry and the modified fly ash slurry after 12 h of standing were 70.8 mPa·s and 63.2 mPa·s, respectively. The plastic viscosity of the modified fly ash slurry was lower than that of fly ash slurry, and its fluidity was better. The plastic viscosities of the fly ash slurry and the modified fly ash slurry after 24 h of standing were 73.2 mPa·s and 81.5 mPa·s, respectively. The plastic viscosity of the fly ash slurry was lower than that of the modified fly ash slurry, which indicates that the flowability of the modified fly ash slurry after 24 h of standing was poor compared with that of the fly ash slurry.

Comparing the changed characteristics of the plastic viscosity of the two different types of slurry over time, the growth rate of the plastic viscosity of the fly ash between 12 h and ca. 24 h was 3.4%, while the growth rate of the plastic viscosity of the modified fly ash slurry was 29%. Therefore, a stage difference was present in the fluidity of the two slurries: the fluidity of the modified fly ash slurry was higher than that of the fly ash slurry within 12 h. After 12 h, the plastic viscosity of the modified fly ash slurry increased rapidly, and the fluidity of the slurry was much lower than that of the fly ash slurry. Therefore, the rheology of the slurry could be changed by adding a 10% mass ratio of cement to the fly ash slurry in order to control the diffusion radius of the slurry, but the rheology of the slurry was significantly affected by time.

3.2. Differences in Diffusion Pattern and Thickness between Fly Ash Slurry and Modified Slurry. Both the fly ash slurry and the modified fly ash slurry had a circular diffusion pattern with the grouting borehole as the center of the circle. The flowability of the fly ash slurry was significantly better than that of the modified fly ash slurry, and its diffusion pattern was irregularly circular. On the other hand, the modified fly ash slurry was less fluid and had a more regular circular diffusion pattern. During the grout filling process, the slurry continuously precipitated, deposited water, and formed solidified ash in the diffusion range. The thickness of the solidified ash was the greatest at the bottom of the filling borehole and decreased along the slurry diffusion direction. The thickness of the ash body in the center of the modified fly ash slurry was always greater than that of the fly ash slurry, and the thickness of the consolidated fly ash slurry was thus lower than that of the consolidated slurry of the modified fly ash under the same conditions of filling slurry volume.

The solidified ash thickness of the fly ash slurry displayed the same trend as the change in the solidified ash thickness of the modified fly ash slurry. As shown in Figure 6, the changes in the deposited ash thickness of both slurries were not obvious until 8 h after the experiment had begun, and the solidified ash thickness also began to increase after 8 h. For the slurry ash thickness, measurements were counted beginning in the 8th hour. The ash thickness of the modified fly ash slurry was always greater than that of the fly ash slurry during the entire experiment. The ash thickness of the two slurries was stabilized at about 2 cm after a large gap beginning at 28 h. In the process of thickness change, both slurries increased more significantly from 50 to 56 h, whereas the slurry diffusion radius changed less, the solidified ash thickness of the process changed quickly, and the slurry diffusion radius changed smoothly.

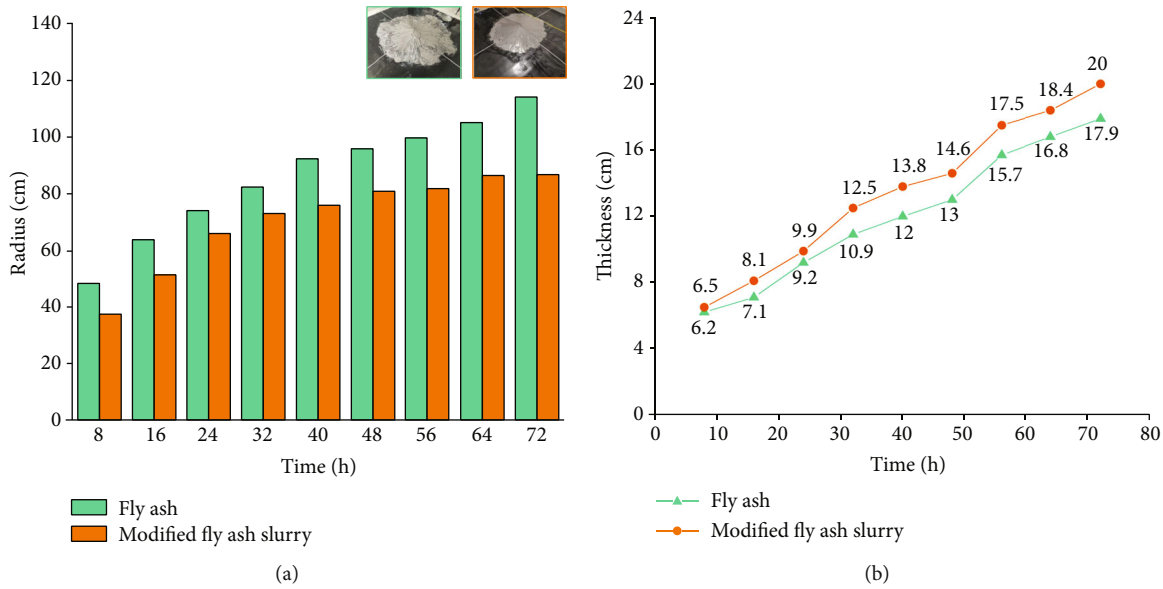

Figure 6: Comparison of slurry flow. (a) Slurry diffusion radius and (b) thickness of deposited slurry.

The volume of the modified fly ash slurry was compared with that of the fly ash slurry when both had reached the same thickness during the experiment. For example, the fly ash body reached an ultimate thickness of 17.9 cm, the fly ash slurry diffusion time was 72 h, and the modified fly ash slurry reached 17.9 cm in 58 h. The calculations reveal that the volume of the modified fly ash slurry filling was 25.2 L less than that of the fly ash slurry, and the volume of saved slurry was 19.4%. Compared with the fly ash slurry, the modified fly ash slurry had a smaller slurry diffusion radius and a greater thickness, which could generate fast support of the strata during the injection (compared with the fly ash slurry).

3.3. Difference in Slurry Diffusion Radius between Fly Ash Slurry and Modified Fly Ash Slurry. According to the experimental results, the slurry diffusion radius of the fly ash slurry from 0 to 3 h increased faster, and its slurry diffusion radius increment gradually decreased after 3 h. The slurry diffusion radius was a power function with the grouting time, and the data can be fitted to obtain the fly ash slurry diffusion radius as a function of time as

$$R_F = 22.15t^{0.38}. \quad (2)$$

Similar to the fly ash slurry, the modified slurry diffusion radius and time were also consistent with the power function relationship, which can be fitted as

$$R_M = 20.47t^{0.35}. \quad (3)$$

Comparing the diffusion radius of the two slurries as a function of time, the coefficient and power index in the slurry diffusion radius function of the fly ash slurry are clearly larger than those of the modified fly ash slurry. In other words, with an increase in grouting time, the inhibiting effect of the modified fly ash slurry on the slurry diffusion radius was much better than that of the fly ash slurry. The longer the grouting time was, the greater the difference between the two diffusion radii was, which fully illustrates the control effect of the modified fly ash slurry on the slurry diffusion radius.

It should be noted that the slurry diffusion radius of the modified fly ash slurry was not always smaller than that of the fly ash slurry. As shown in Figure 7, the slurry diffusion radius of the modified fly ash slurry was greater than the diffusion radius of the fly ash slurry during the 0–20 min grouting process, and the diffusion radius of the fly ash slurry began to become greater than that of the modified fly ash slurry after the 20th min of grout filling. The diffusion radius of the fly ash slurry far exceeded that of the modified fly ash slurry during the subsequent grouting process.

Therefore, the effect of the modified fly ash slurry on the control of the diffusion radius was mainly reflected after 20 min as shown in Figure 8, from the 20th min to the end of the grouting (20 min~72 h), and the difference in the diffusion radius between the two slurries gradually increased. Compared with the fly ash slurry, the modified fly ash slurry diffusion radius could be reduced by 19.43% on average.

3.4. Mechanism of Inhibition of Diffusion Radius of Modified Fly Ash Slurry. As shown in Figure 9, compared with fly ash slurry, the diffusion of the modified fly ash slurry can be divided into 2 stages: a "stability control stage" and a "consolidation control stage."

The stability control stage occurred during the early stage of the slurry diffusion (0~20 min). Due to the addition of cement, the slurry contained tricalcium aluminate ($3CaO{\cdot}Al_2O_3$), which enhanced the water absorption capacity of the modified fly ash slurry, and both slurry stability and fluidity thus improved. Therefore, the diffusion radius

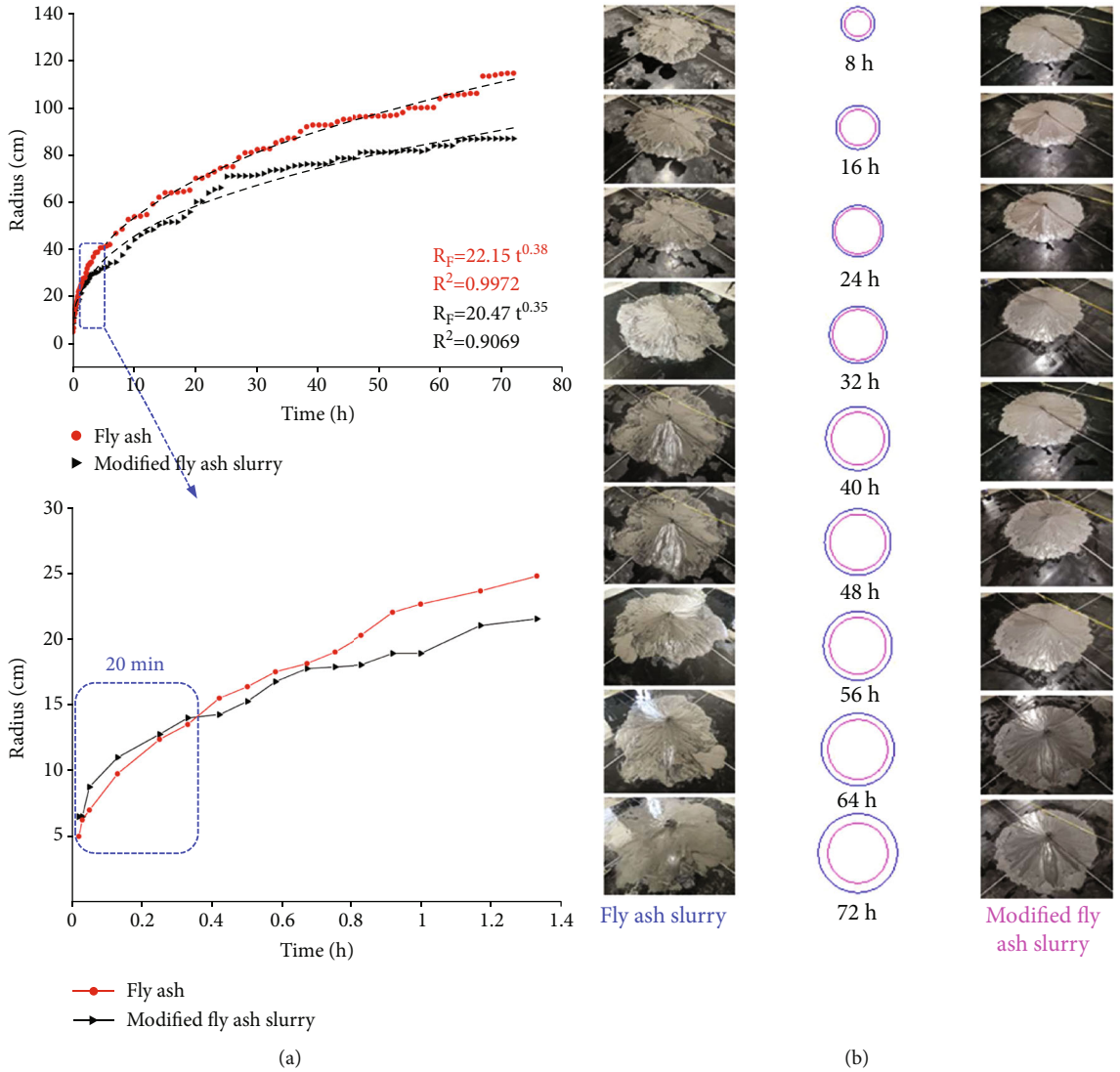

Figure 7: Difference in diffusion radius of fly ash slurry and modified fly ash slurry. (a) Entire process of fly ash slurry and modified fly ash slurry diffusion and (b) fly ash slurry and modified fly ash slurry diffusion distance and diffusion pattern.

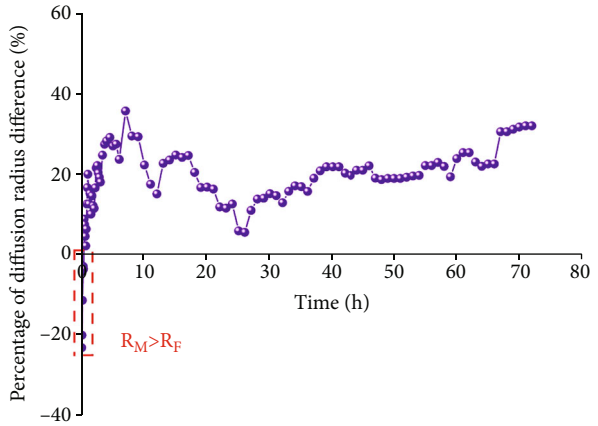

Figure 8: Percentage of diffusion radius difference.

of the modified fly ash slurry was greater than that of the fly ash slurry from 0 to 20 min.

The curing control stage occurred after 20 min, mainly because the modified fly ash slurry continued to harden and generate strength, which made the diffusion radius of the modified fly ash slurry smaller than that of the fly ash slurry. The slurry diffusion radius gap became more obvious with increasing grouting time.

It should be noted that the diffusion radius of both slurries displayed a significant difference after 45 min, and the solidifying action became more and more significant due to the initial setting time of the cement (i.e., 40–45 min). Therefore, the cementation stage of the modified fly ash slurry that had been made by adding cement to the fly ash occurred mainly after the cement had reached the initial setting time, which also caused the thickness of the cemented ash body of the modified fly ash slurry to far exceed the thickness of the fly ash body.

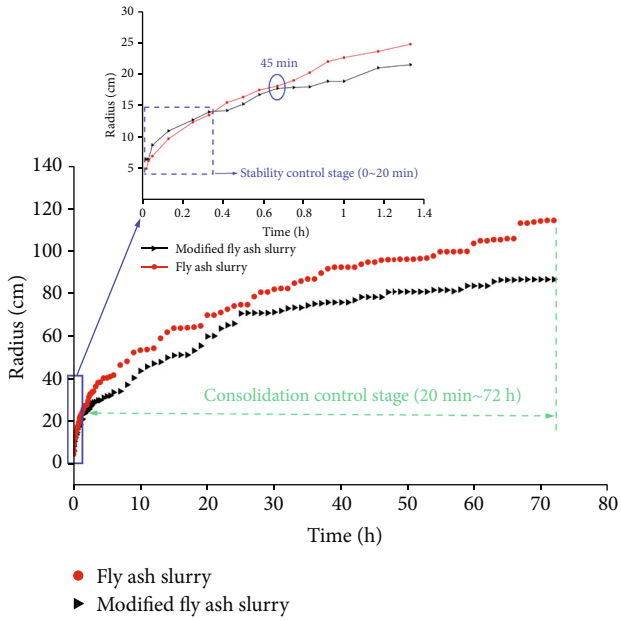

Figure 9: Two-stage effect of diffusion radius of modified fly ash slurry.

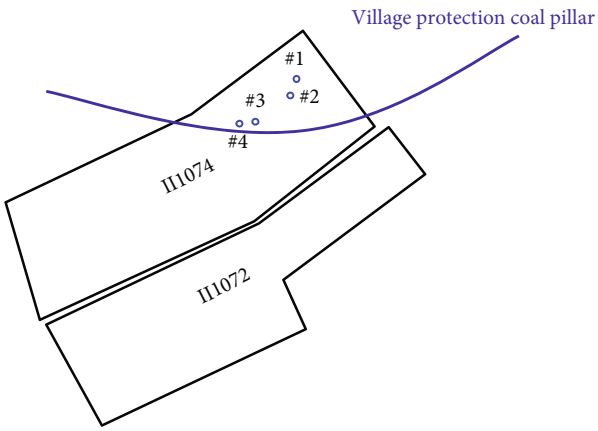

Figure 10: Plan view of II1074 longwall panel.

4. Field Investigation

Yangliu coal mine is located in Huaibei, Anhui Province, China. Longwall panel II1074 mines seam #10 with a thickness of 3.4 m. The panel width is 210 m, and the length is 700 m. As shown in Figure 10, in order to protect the surface buildings, it is necessary to implement grout filling about 350 m range from the working face, but the outer section does not need to be grouted. In order to control the spread of the slurry during our test, modified fly ash slurry was used.

There are 4 surface holes in the working face. Through the implementation of grout filling, a total of 89,638 t of fly ash was filled, and 2,800 t of cement was mixed. During the grouting process, cement was added in order to modify the slurry in boreholes #1, #3, and #4, but not in borehole #2. During the grouting process, the borehole pressure was continuously monitored in order to evaluate the effect of the modified fly ash slurry.

Monitoring revealed that the pressure in the filling cavity increased more quickly after using the modified fly ash slurry. As shown in Figure 11(a), both boreholes #1 and #3 were initially filled with fly ash slurry, but always in a pressure-free state. When grouting with modified fly ash slurry with a 10% cement-mixing ratio, the pressure in borehole #1 increased rapidly from 0.07 MPa to 1.59 MPa, and the pressure in borehole #3 increased rapidly from 1 MPa to 4 MPa.

As a comparison, the duration of the low-pressure stage of the borehole was longer when using the fly ash slurry. Figure 11(a) shows that the longwall advance distance during the time that borehole #2 reached the ultimate pressure from zero was 382 m, and the accumulated filling volume was 29,026 t. The longwall advance distance for borehole #4 was 283 m, and the accumulated filling volume was 23,900 t.

This comparison reveals that the slurry diffusion radius could be shortened by 26%, and the filling volume reduced by 18% after using the modified fly ash slurry with a 10% cement-mixing ratio. Under the same conditions of injection volume, the borehole could be pressurized more quickly after using the modified fly ash slurry. As shown in Figure 11(b), at a single borehole filling volume of 12,000 t, the grouting pressure of boreholes #1, #3, and #4 with the modified fly ash slurry were 0.5, 1.6, and 1.2 MPa, respectively, which represented an average increase of 37.5% compared with the grouting pressure of 0.8 MPa for boreholes with nonmodified fly ash slurry. At a single borehole filling volume of 16,000 t, the grouting pressures of boreholes #1, #3, and #4 with the modified fly ash slurry were 1.4 MPa. The grouting pressure of boreholes #1, #3, and #4 with the modified fly ash slurry were 1.4, 4, and 1.5 MPa, respectively, which increased by 91.7% on average compared with the grouting pressure of 1.2 MPa in the boreholes with the nonmodified fly ash slurry. This finding indicates that the modified fly ash slurry effectively controlled the slurry diffusion radius.

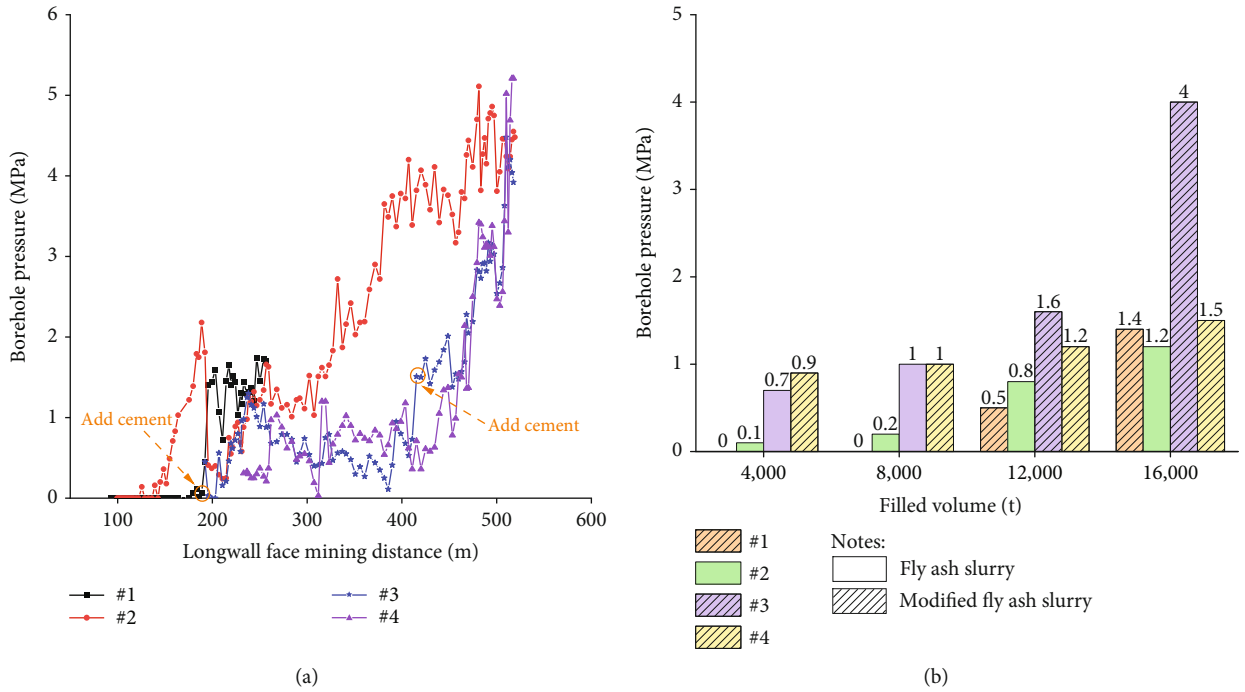

FIGURE 11: Grouting pressure variation. (a) Boreholes #1–4 and (b) borehole pressure at same injection volume of modified fly ash slurry and fly ash slurry.

5. Conclusions

The generation and propagation of mining-induced overburden fractures plays a vital role in surface subsidence for longwall mining engineering. Overburden isolated grouting achieves control of surface subsidence by filling overburden fractures. Controlling the slurry diffusion radius is fundamental to grouting, which is important in partial grouting engineering. When the local area of a longwall panel needs to be grouted, the traditional fly ash slurry allows a large diffusion beyond the expected range, leading to unnecessary grout take and cost. This paper proposed a method of adding cement to fly ash slurry in order to suppress the diffusion radius and reduce unnecessary grout take. Through experimental methods, the basic characteristic parameters of the modified slurry were measured. An experimental slurry flow simulation system was constructed, an experimental study of the diffusion radius of the modified slurry was carried out, and the mechanism of action of the modified slurry for controlling the diffusion radius was discussed.

The study found that there were differences in the degree of influence of the water-ash ratio and the cement ratio on the basic properties of the modified slurry. The cement-mixing ratio (i.e., 10%, 20%, 50%, and 80%) had less effect on the density of the modified slurry, which almost did not change with the changing cement ratio. However, the effect on the precipitation rate and viscosity of the slurry was significant, and the precipitation rate varied greatly under different cement-mixing ratio conditions. Comparing the changed characteristics of the plastic viscosity of the two different types of slurry over time, the growth rate of the plastic viscosity of the fly ash between 12 h and ca. 24 h was 3.4%, while the growth rate of the plastic viscosity of the modified fly ash slurry was 29%.

An experimental study on the diffusion of modified slurry and fly ash slurry was carried out and revealed that the diffusion morphology of both the fly ash slurry and the modified fly ash slurry showed circular diffusion centered around the grouting borehole, but the modified slurry had poor mobility and large solidified ash thickness. Moreover, the study found a stage characteristic of the difference in diffusion distance between the fly ash slurry and the modified fly ash slurry, and the inhibition effect of the modified slurry on the diffusion radius gradually increased over time. Compared with the traditional slurry, the volume of the filled modified slurry with 10% cement-mixing ratio was reduced by 19.4% for the same fill thickness. Finally, the study additionally found that the diffusion radius of the modified slurry was 19.43% lower than that of the fly ash slurry over 72 h of continuous experimentation. This finding fully illustrates the control effect of the modified slurry on the diffusion radius.

The inhibition process of the modified slurry on the diffusion radius was reflected in both the stability control stage and the consolidation control stage. Within the stability control stage, the slurry had enhanced water absorption capacity, which caused it to have better diffusion ability, as manifested in the larger modified slurry diffusion radius compared with that of the fly ash slurry. In essence, during the consolidation control stage, the cement gradually began to solidify and harden when it had reached the initial setting time, which significantly reduced the diffusion radius of the slurry during cement consolidation and hardening and also caused the thickness of the consolidated ash body of the modified slurry to far exceed the thickness of the fly ash body.

Based on these experimental research results, field tests were conducted in the local area grouting project of the Yangliu coal mine in Huaibei, Anhui Province, China. Using a modified slurry with a 10% cement-blending ratio for grout filling, the diffusion radius of the slurry and the filling volume was found to be reduced by 26% and 18%, respectively. The modified slurry caused the grouting pressure in the borehole to rise faster and effectively controlled the slurry diffusion range, thereby reducing the grout filling volume and improving the grouting effect.

Data Availability

The research data used to support the findings of the present study may be released upon reasonable request addressed to the corresponding author, who can be contacted at li_jian@cumt.edu.cn. Some or all of the data, models, or code generated or used during the study are available upon reasonable request addressed to the corresponding author.

Conflicts of Interest

The authors declare that there are no conflicts of interest regarding the publication of this paper.

Acknowledgments

This work was supported by the Fundamental Research Funds for the Central Universities (2020ZDPYMS15).

References

[1] V. Palchik, "Experimental investigation of apertures of mining-induced horizontal fractures," *International Journal of Rock Mechanics and Mining Sciences*, vol. 47, no. 3, pp. 502–508, 2010.

[2] T. Kuang, Z. Li, B. Zhu et al., "The impact of key strata movement on ground pressure behaviour in the Datong coalfield," *International Journal of Rock Mechanics and Mining Sciences*, vol. 119, pp. 193–204, 2019.

[3] J. Xu and M. Qian, "Study on the distribution characteristics of mining-induced fractures in overburden," *Ground Pressure and Strata Control*, vol. 3, pp. 213–215, 1997.

[4] H. Yavuz, "An estimation method for cover pressure re-establishment distance and pressure distribution in the goaf of longwall coal mines," *International Journal of Rock Mechanics and Mining Sciences*, vol. 41, no. 2, pp. 193–205, 2004.

[5] Q. Hu, X. Deng, R. Feng, C. Li, X. Wang, and T. Jiang, "Model for calculating the parameter of the Knothe time function based on angle of full subsidence," *International Journal of Rock Mechanics and Mining Sciences*, vol. 78, pp. 19–26, 2015.

[6] J. Ju and J. Xu, "Surface stepped subsidence related to top-coal caving longwall mining of extremely thick coal seam under shallow cover," *International Journal of Rock Mechanics and Mining Sciences*, vol. 78, pp. 27–35, 2015.

[7] F. Meng, C. Piao, B. Shi, T. Sasaoka, and H. Shimada, "Calculation model of overburden subsidence in mined-out area based on Brillouin optical time-domain reflectometer technology," *International Journal of Rock Mechanics and Mining Sciences*, vol. 138, article 104620, 2021.

[8] J. Xu and M. Qian, "Study and application of mining-induced fracture distribution in green mining," *Journal of China University of Mining & Teehnology*, vol. 2, pp. 17–20, 2004.

[9] J. Ju and J. Xu, "Structural characteristics of key strata and strata behaviour of a fully mechanized longwall face with 7.0 m height chocks," *International Journal of Rock Mechanics and Mining Sciences*, vol. 58, pp. 46–54, 2013.

[10] X. Wang, F. Xiao, Q. Zhang, A. Zhou, and R. Liu, "Grouting characteristics in rock fractures with rough surfaces: apparatus design and experimental study," *Measurement*, vol. 184, article 109870, 2021.

[11] J. Ju, J. Xu, Y. Liu et al., "Key strata movement monitoring during underground coal mining and its 5-stage movement law inversion: a case study in Hong Qinghe mine," *Journal of China Coal Society*, vol. 47, pp. 611–622, 2022.

[12] J. Xu, D. Xuan, W. Zhu, X. Wang, B. Wang, and H. Teng, "Study and application of coal mining with partial backfilling," *Journal of China Coal Society*, vol. 40, pp. 1303–1312, 2015.

[13] J. Xu, D. Xuan, W. Zhu, and X. Wang, "Partial backfilling coal mining technology based on key strata control," *Journal of Mining and Strata Control Engineering*, vol. 1, p. 13504, 2019.

[14] J. Xu, "Research and progress of coal mine green mining in 20 years," *Coal Science and Technology*, vol. 48, pp. 1–15, 2020.

[15] J. Xu, W. Qin, D. Xuan, and W. Zhu, "Accumulative effect of overburden strata expansion induced by stress relief," *Journal of China Coal Society*, vol. 45, pp. 35–43, 2020.

[16] D. Xuan and J. Xu, "Grout injection into bed separation to control surface subsidence during longwall mining under villages: case study of Liudian coal mine, China," *Natural Hazards*, vol. 73, no. 2, pp. 883–906, 2014.

[17] D. Xuan, J. Xu, and W. Zhu, "Dynamic disaster control under a massive igneous sill by grouting from surface boreholes," *International Journal of Rock Mechanics and Mining Sciences*, vol. 71, pp. 176–187, 2014.

[18] D. Xuan, J. Xu, B. Wang, and H. Teng, "Investigation of fill distribution in post-injected longwall overburden with implications for grout take estimation," *Engineering Geology*, vol. 206, pp. 71–82, 2016.

[19] D. Xuan and J. Xu, "Longwall surface subsidence control by technology of isolated overburden grout injection," *International Journal of Mining Science and Technology*, vol. 27, no. 5, pp. 813–818, 2017.

[20] D. Xuan, J. Li, K. Zheng, and J. Xu, "Experimental study of slurry flow in mining-induced fractures during longwall overburden grout injection," *Geofluids*, vol. 2020, Article ID 8877616, 10 pages, 2020.

[21] D. Xuan, J. Xu, B. Wang, and H. Teng, "Borehole investigation of the effectiveness of grout injection technology on coal mine subsidence control," *Rock Mechanics and Rock Engineering*, vol. 48, no. 6, pp. 2435–2445, 2015.

[22] D. Xuan, B. Wang, and J. Xu, "A shared borehole approach for coal-bed methane drainage and ground stabilization with grouting," *International Journal of Rock Mechanics and Mining Sciences*, vol. 86, pp. 235–244, 2016.

[23] B. Wang, J. Xu, and D. Xuan, "Time function model of dynamic surface subsidence assessment of grout-injected overburden of a coal mine," *International Journal of Rock Mechanics and Mining Sciences*, vol. 104, pp. 1–8, 2018.

[24] L. Zhang, J. Xu, D. Xuan, and M. Gan, "Experimental and applied research on compression properties of slurry used for isolated overburden grout injection," *Journal of China Coal Society*, vol. 42, pp. 1117–1122, 2017.

[25] L. Zhang, J. Xu, and D. Xuan, "Experimental research on slurry bleeding properties of isolated grouting filling for overburden," *China Coal*, vol. 43, pp. 121–124, 2017.

[26] Y. Tian, Q. Liu, H. Ma, Q. Liu, and P. Deng, "New peak shear strength model for cement filled rock joints," *Engineering Geology*, vol. 233, pp. 269–280, 2018.

[27] S. Li, D. Pan, Z. Xu, P. Lin, and Y. Zhang, "Numerical simulation of dynamic water grouting using quick-setting slurry in rock fracture: the sequential diffusion and solidification (SDS) method," *Computers and Geotechnics*, vol. 122, article 103497, 2020.

[28] X. Liu, C. Hu, Q. Liu, and J. He, "Grout penetration process simulation and grouting parameters analysis in fractured rock mass using numerical manifold method," *Engineering Analysis with Boundary Elements*, vol. 123, pp. 93–106, 2021.

[29] J. Ren, H. Zhao, L. Zhang et al., "Design optimization of cement grouting material based on adaptive boosting algorithm and simplicial homology global optimization," *Journal of Building Engineering*, vol. 49, article 104049, 2022.

[30] H. Jahangir, A. Soleymani, and M. R. Esfahani, "Investigating the confining effect of steel reinforced polymer and grout composites on compressive behavior of square concrete columns," *Iranian Journal of Science and Technology, Transactions of Civil Engineering*, vol. 2022, pp. 1–17, 2022.

[31] C. Wang, D. Zhang, H. Chen, H. Zhang, X. Xiao, and Z. Liu, "Preparation and properties of silicon-modified epoxy grouting material for repairing microcracks," *Journal of Materials in Civil Engineering*, vol. 34, no. 3, p. 04021479, 2022.

[32] Y. Deng, X. Yue, S. Liu, Y. Chen, and D. Zhang, "Hydraulic conductivity of cement-stabilized marine clay with metakaolin and its correlation with pore size distribution," *Engineering Geology*, vol. 193, pp. 146–152, 2015.

[33] H. Sun, Z. Weng, S. Liu et al., "Compression and consolidation behaviors of lime-treated dredging slurry under vacuum pressure," *Engineering Geology*, vol. 270, article 105573, 2020.

[34] R. Chu, Y. Li, X. Meng et al., "Research on the slurrying performance of coal and alkali-modified sludge," *Fuel*, vol. 294, p. 120548, 2021.

[35] D. Yao, H. Zhao, Z. Chen, and H. Liu, "Preparation of high concentration coal water slurry with good fluidity based on only modified fine particles under bimodal distribution using the second fluid and the second particle," *Fuel*, vol. 317, article 123461, 2022.